NeuroImage: Clinical 30 (2021) 102532

Contents lists available at ScienceDirect

NeuroImage: Clinical

journal homepage: www.elsevier.com/locate/ynicl

# An fMRI investigation of neural activation predicting memory formation in children with fetal alcohol spectrum disorders

Catherine E. Lewis [a,b,*], Kevin G.F. Thomas [a], Noa Ofen [c], Christopher M.R. Warton [b], Frances Robertson [d], Nadine M. Lindinger [a,b], Christopher D. Molteno [e], Ernesta M. Meintjes [d], Joseph L. Jacobson [b,e,f], Sandra W. Jacobson [b,e,f,*]

[a] ACSENT Laboratory, University of Cape Town, Faculty of Humanities, Department of Psychology, Cape Town, South Africa
[b] Child Development Research Laboratory, University of Cape Town, Faculty of Health Sciences, Department of Human Biology, Cape Town, South Africa
[c] Life-Span Cognitive Neuroscience Program, Institute of Gerontology, Wayne State University, Department of Psychology, Detroit, MI, USA
[d] MRC/UCT Medical Imaging Research Unit, University of Cape Town, Division of Biomedical Engineering, Department of Human Biology, Cape Town, South Africa
[e] Child Development Research Laboratory, University of Cape Town, Faculty of Health Sciences, Department of Psychiatry and Mental Health, Cape Town, South Africa
[f] Child Development Research Laboratory, Wayne State University School of Medicine, Department of Psychiatry and Behavioral Neurosciences, Detroit, MI, USA

ARTICLE INFO

*Keywords:*
Fetal alcohol spectrum disorders
Prenatal alcohol exposure
fMRI
Memory encoding
Memory formation
Subsequent memory formation

ABSTRACT

Prenatal alcohol exposure (PAE) is associated with physical anomalies, growth restriction, and a range of neurobehavioral deficits. Although declarative memory impairment has been documented extensively in individuals with fetal alcohol spectrum disorders (FASD), this cognitive process has been examined in only one functional magnetic resonance imaging (fMRI) study, and mechanisms underlying this impairment are not well understood. We used an event-related fMRI design to examine neural activations during visual scene encoding that predict subsequent scene memory in 51 right-handed children (age range = 10–14 years, $M = 11.3$, SD = 1.3) whose mothers had been recruited and interviewed prospectively about their alcohol use during pregnancy. Following examination by expert dysmorphologists, children were assigned to one of three FASD diagnostic groups: FAS/PFAS ($n_{FAS} = 7$; $n_{PFAS} = 4$), nonsyndromal heavily exposed (HE; $n = 14$), and Controls ($n = 26$). Subsequent memory was assessed in a post-scan recognition test, and subsequent memory activations were examined by contrasting activations during encoding of scenes that were subsequently remembered (hits) to those for incorrectly judged as 'new' (misses). Recognition accuracy did not differ between groups. Pooled across groups, we observed extensive bilateral subsequent memory effects in regions including the hippocampal formation, posterior parietal cortex, and occipital cortex—a pattern consistent with previous similar studies of typically developing children. Critically, in the group of children with FAS or PFAS, we observed activations in several additional regions compared to HE and Control groups. Given the absence of between-group differences in recognition accuracy, these data suggest that in achieving similar memory compared to children in the HE and Control groups, children with FAS and PFAS recruit more extensive neural resources to achieve successful memory formation.

## 1. Introduction

Prenatal alcohol exposure (PAE) is associated with physical anomalies, growth restriction, and a range of neurobehavioral deficits. According to the Revised Institute of Medicine guidelines(Hoyme et al., 2005), fetal alcohol syndrome (FAS), the most severe of the fetal alcohol spectrum disorders (FASD), is diagnosed when three criteria are met: (a) a specific pattern of craniofacial dysmorphology (including short palpebral fissures, thin upper lip, and smooth philtrum), (b) growth restriction (height or weight $\leq$ 10th percentile), and (c) small head circumference ($\leq$10th percentile). Partial FAS (PFAS) is diagnosed when cranio-facial features are present together with growth restriction or small head circumference and confirmation of maternal alcohol consumption during pregnancy. Some of the highest FASD prevalence rates (estimated at 135–208 cases/1000 for school-aged children [May et al.,

* Corresponding authors at: Child Development Research Laboratory, University of Cape Town, Faculty of Health Sciences, Department of Human Biology, Anzio Road, Observatory, Cape Town, RSA (C.E. Lewis); Child Development Research Laboratory, Wayne State University School of Medicine, Department of Psychiatry and Behavioral Neurosciences, 3901 Chrysler Drive, Detroit, MI 48201, USA (S.W. Jacobson).
*E-mail addresses:* catherine.lewis.04@gmail.com (C.E. Lewis), sandra.jacobson@wayne.edu (S.W. Jacobson).

https://doi.org/10.1016/j.nicl.2020.102532
Received 16 June 2020; Received in revised form 7 December 2020; Accepted 8 December 2020
Available online 11 December 2020

2013]) are reported in economically disadvantaged communities in the Western Cape province of South Africa (Roozen et al., 2016).

Neuropsychological studies designed to characterize the neurocognitive profile of FASD have identified declarative memory as particularly vulnerable to the effects of heavy PAE (Mattson et al., 2019). Several studies of verbal learning and memory have attempted to tease apart component processes (e.g., encoding and retrieval) that are integral to effective declarative memory performance (du Plooy et al., 2016; Lewis et al., 2015). Some of these studies have reported that children with heavy PAE show a pattern of impaired information acquisition alongside spared retention and retrieval of information(Crocker et al., 2011; Kaemingk et al., 2003; Lewis et al., 2015; Mattson et al., 1996; Mattson and Roebuck, 2002; Pei et al., 2008). However, in two recent studies children with moderate PAE displayed impaired performance at both encoding and retrieval stages (Gross et al., 2017; Lewis et al., 2015). These studies suggest that previously observed absences of a PAE effect on retrieval may have been due to the failure of more heavily exposed children to encode a sufficient number of stimuli to permit valid assessment of their retrieval abilities. The current study used functional neuroimaging to examine the mechanisms underlying learning and memory impairments in children with PAE to further clarify the effects of PAE on memory-related processes of encoding and retrieval.

Only one previous study has used functional magnetic resonance imaging (fMRI) to directly assess neural activation during memory encoding and retrieval in an FASD sample (heavy PAE $n = 11$; Control $n = 16$; Sowell et al., 2007). To examine memory-related activation, Sowell et al. (2007) compared levels of regional brain activation combined across learning and recall trials vs. that observed during baseline rest periods. When compared to Control participants, those with PAE showed decreased activation in temporal regions known to be activated during memory encoding and retrieval and increased activation in the left dorsolateral prefrontal cortex (PFC). These findings are consistent with other task-based fMRI studies of FASD in suggesting that exposed children often recruit alternative networks, apparently to compensate for a functional deficit in the network normally used to perform the task (e.g., Diwadkar et al., 2013; Fryer et al., 2007a; Meintjes et al., 2010; Kodali et al., 2017; Ware et al., 2015). Because learning and recall trials were combined in the Sowell et al. study, it was not possible to distinguish between alterations in neural activation patterns associated with encoding vs. retrieval of information. Their findings, therefore, warrant follow-up investigation using a paradigm designed to differentiate between these two memory-related processes.

The event-related fMRI *subsequent memory* paradigm (Brewer et al., 1998; Wagner et al., 1998) assesses neural activation patterns during encoding that predict successful memory formation. Although this paradigm has been used frequently in healthy young adults (Kim, 2011), only a few studies have used it in pediatric samples. In one of the earliest such studies, Ofen et al. (2007) examined a sample of 49 right-handed typically developing participants (8–24 yr) and detected neural activation in several of the same medial temporal lobe (MTL) and PFC regions associated with successful memory formation in adult samples (see Kim, 2011). Few studies have used the subsequent memory paradigm to investigate neural activations predicting successful memory formation in clinical pediatric samples (e.g., Krauel et al., 2007), and there has been no application of this paradigm in the FASD literature.

The present study used an event-related fMRI subsequent memory paradigm (Ofen et al., 2007) to investigate neural activations during the encoding of visual scenes that predicted successful memory formation in a sample of school-aged children with and without a history of heavy PAE. We hypothesized that (1) the pattern of brain activation predicting successful memory formation for the sample as a whole (i.e., in children with and without heavy PAE) would resemble that reported in previous studies using the subsequent memory paradigm; (2) children with heavy PAE would recruit a more extensive subsequent memory neural network than Controls; and (3) higher levels of PAE would be correlated with greater differences in magnitude of activation within the subsequent memory clusters, in a dose-dependent fashion.

## 2. Methods

### 2.1. Participants

We assessed 78 right-handed school-aged children from the Cape Town Longitudinal Cohort (Jacobson et al., 2008). Consent and study procedures were approved by the relevant research ethics committees of Wayne State University and the University of Cape Town (UCT).

The children's mothers were recruited during pregnancy between 1999 and 2002 from a local antenatal clinic in Cape Town, South Africa, that serves an economically disadvantaged, predominantly Cape Coloured (mixed ancestry) community in which heavy drinking during pregnancy is highly prevalent(Croxford and Viljoen, 1999; May et al., 2013). At recruitment, a research nurse used a timeline follow-back (TLFB) approach (Jacobson et al., 2002) to interview the mother about her alcohol consumption. The interview was adapted to include information about the type of beverage consumed and about sharing (size of container shared by how many women) to reflect how many pregnant women in this community drink (Jacobson et al., 2008, 2017). Alcohol use was also ascertained in two subsequent TLFB interviews: one covering a 2-week period in mid-pregnancy and the other, at 1-month postpartum, assessing a typical 2-week period during the later part of pregnancy.

For each type of alcoholic beverage consumed, volume consumed each day was recorded and converted to oz of absolute alcohol (AA), using the following weights: liquor = 0.4, beer = 0.05, wine = 0.12, cider = 0.06 (adapted from Bowman et al., 1975, to reflect values for beer, wine and hard liquor sold in Cape Town at the time of recruitment). Data from the three TLFB interviews were then averaged to provide these summary measures of PAE: oz AA/day averaged across pregnancy, oz AA/drinking day, and frequency (drinking days/week). We have previously validated this TLFB interview in relation to fatty acid ethyl esters (FAEEs) and biologically stable metabolites of alcohol that are deposited in meconium (Bearer et al., 2003), as well as to infant outcomes (Jacobson et al., 2002). The women were also asked how many cigarettes/day they smoked and how many days/month they used marijuana, methaqualone or cocaine.

Mothers were invited to participate if they reported drinking heavily during pregnancy (at least 1 oz AA [equivalent of ~2 standard drinks]/day or engaged in binge drinking [≥5 standard drinks/occasion]). Controls were women from the same community and antenatal clinics who abstained from alcohol use during pregnancy or who drank only minimally. All women who reported drinking during pregnancy were advised to stop or reduce their alcohol intake and were offered a referral for help to do so. Women <18 yr of age and those with diabetes, epilepsy, or cardiac problems requiring treatment were excluded. Infant exclusionary criteria were major chromosomal anomalies, neural tube defects, multiple births, and seizures.

In 2005 we organized a clinic in the community, in which the children were examined for FAS dysmorphology and growth using a standard protocol that included assessment of features, such as palpebral fissure length, philtrum and vermilion (Hoyme et al., 2005). The protocol was administered independently by two internationally recognized experts in FASD diagnosis, H.E. Hoyme, M.D. (HEH) and L.K. Robinson, M.D. (LKR), who were blind regarding maternal alcohol history (Jacobson et al., 2008). FAS and PFAS diagnoses were determined from the examiners' protocols at case conferences by HEH, LKR, SWJ, JLJ, and CDM. The diagnoses were subsequently confirmed by examinations conducted in follow-up clinics in 2009, 2013, and 2016. Each participant was assigned to one of three FASD diagnostic groups: FAS/PFAS ($n_{FAS} = 11$; $n_{PFAS} = 10$), nonsyndromal heavily exposed (HE; $n = 24$), and Controls ($n = 33$).

Mothers were interviewed about their sociodemographic background by a developmental pediatrician (CDM). All maternal interviews and child neuropsychological assessments were conducted at the UCT

Child Development Research Laboratory. General intellectual functioning was assessed using the Wechsler Intelligence Scales for Children-Fourth Edition (WISC-IV; Wechsler, 2003). Handedness was assessed using the Edinburgh Handedness Inventory (Oldfield, 1971). Only right-handed children were included in the present study to avoid introducing heterogeneity due to differences in brain lateralization. Attention deficit hyperactivity disorder (ADHD) was assessed using research criteria (see Jacobson et al., 2011) based on rating scales completed by the child's mother, teacher, and the examiner, which provided the basis for a DSM-IV (American Psychiatric Association, 1994) diagnosis. At each neuropsychological and neuroimaging visit, mothers and children were provided with breakfast, a snack, and/or lunch. Additionally, mothers were given a small financial compensation, and children were given a small gift following each assessment.

### 2.2. Neuroimaging assessment

The data were collected and processed by individuals blind regarding participant alcohol exposure history and FASD diagnoses.

#### 2.2.1. Magnetic resonance imaging protocol

Mothers and children were transported by our research driver and nurse to the Cape Universities Brain Imaging Centre (CUBIC) for scanning. Each child was scanned, using a single-channel head coil, on a 3 T Allegra MR scanner (Siemens, Erlangen, Germany).

High-resolution $T_1$-weighted magnetization-prepared rapid gradient echo (MPRAGE) anatomical scans were acquired in a sagittal orientation using a three-dimensional motion corrected multi-echo sequence(Tisdall et al., 2009; van der Kouwe et al., 2008), with the following parameters: TR 2530 ms, TEs 1.53/3.21/4.89/6.57 ms, 128 slices, slice thickness 1.3 mm, flip angle 7°, field of view 256 mm, voxel size 1.3 × 1.0 × 1.3 $mm^3$, and scan time 8:07 min. Each of the three encoding sessions followed the same fMRI acquisition protocol. Specifically, within each session, 124 functional $T_2$*-weighted volumes sensitive to blood-oxygen level dependent (BOLD) contrast were acquired using a gradient echo, echo planar sequence with the following parameters: TR 2000 ms, TE 30 ms, 34 slices, slice thickness 3 mm, flip angle 90°, field of view 200 mm, voxel size 3.1 × 3.1 × 3.0 $mm^3$, and scan time 4:12 min.

#### 2.2.2. Functional magnetic resonance imaging experimental task

We used an event-related fMRI design to assess patterns of neural activation during visual scene encoding that predict subsequent scene memory. The subsequent memory paradigm (Ofen et al. 2007, Tang et al. 2018) is divided into two parts: (a) the in-scanner encoding phase, and (b) the post-scan recognition memory test. Both parts were programmed and run in E-Prime 2.0 (Psychology Software Tools, Inc., Pittsburgh, USA). Each child practiced the in-scanner task and post-test in a mock scanner, which has been shown to help reduce anxiety and facilitate completion of high-quality MRI scans(Hallowell et al., 2008). The child was informed that that their memory for the task stimuli would be assessed following the scan.

During the in-scanner encoding phase, 120 novel images of indoor and outdoor scenes were presented across 3 runs (40 images per run). To allow for counterbalancing across participants and between target and foil conditions, task stimuli were arranged in six lists of 40 images (20 indoor and 20 outdoor scenes). Each child was assigned a selection of 3 of the 6 possible lists. Within each run, stimuli from a single list were presented in a randomized order and were displayed for 3 s with a jittered interstimulus interval (range: 0.5–12.5 s). A fixation cross was displayed for the duration of the interstimulus interval. To help maintain the children's attention during encoding, for each stimulus presented during the scanner phase the participant was instructed to press a button using his/her right-hand index finger to indicate if the image was of an indoor scene or right-hand middle finger to indicate if it was an outdoor scene. Those images that were incorrectly judged were excluded from the neuroimaging analyses to reduce the effect of variations in attention on the analysis of subsequent memory effects. Four children judged >10% of the images incorrectly, with no >25 of the 120 images (21%) judged incorrectly by any one participant ($M = 3.3$, SD = 4.8). Inclusion of the images that were incorrectly judged did not change the overall results. The duration of each encoding run was 4 min.

The post-scan recognition memory test consisted of 200 images of indoor and outdoor scenes: 120 target images (i.e., those presented earlier, during the in-scanner encoding sessions) and 80 new foil images. Participants were asked to indicate whether or not they recognized each scene as a target image. The task was self-paced, and the examiner entered the child's response on the computer. Foil scenes were drawn from the remaining image lists that had not been presented to the participant in the scanner. Target and foil scenes were presented in a random order across three blocks, with a self-paced inter-block break.

Based on the responses during the recognition memory test, each of the 120 target images was classified as either a *hit* (i.e., target scene subsequently remembered as 'old') or a *miss* (i.e., target scene incorrectly judged as 'new'). Further, each of the 80 foil images was classified as either a *false alarm* (i.e., foil scene incorrectly judged as 'old') or a *correct rejection* (i.e., foil scene correctly judged as 'new'). The subsequent memory paradigm is designed to yield a similar number of hit and miss trials across participants (Ofen et al., 2007; Chai et al., 2014; Tang et al., 2018; 2020). Having included fewer foil than target scenes in the post-scan recognition memory test, we recorded roughly equal numbers of 'old' (hits and false alarms) and 'new' (miss and correct rejection) responses from participants. This design enabled us to calculate a robust subsequent memory contrast that is independent of response bias. Neural activation associated with successful memory formation was operationally defined as greater activation for target scenes subsequently remembered as 'old' than for target scenes incorrectly judged as 'new' (Hit > Miss).

### 2.3. Data analysis

All but 1 of 78 participants completed the entire neuroimaging assessment. The exception was a 10-year-old boy in the FAS/PFAS group, who was behaviorally non-compliant during the in-scanner encoding phase. Of the 77 children who completed the neuroimaging assessment, imaging data for 20 children (FAS/PFAS: $n_{FAS} = 3$, $n_{PFAS} = 3$, HE: $n = 10$, Control: $n = 4$) were excluded due to excessive movement (i.e., > 3 mm displacement or 3° rotation) and for an additional 6 (PFAS: $n = 4$; Control: $n = 3$) due to post-test performance at chance levels (i.e., guessing; *d*-prime < 0.25). Results are, therefore, presented for a final study sample of 51 participants (FAS/PFAS: $n_{FAS} = 7$, $n_{PFAS} = 4$; HE: $n = 14$; Control: $n = 26$).

#### 2.3.1. Initial analyses of neuroimaging data

*2.3.1.1. Preprocessing.* Functional MRI data were processed using SPM8 (Wellcome Department of Imaging and Neuroscience, London, UK). The first four volumes were discarded from all analyses to allow for $T_1$ equilibration. Preprocessing included manual orientation to the AC-PC line, correction for interleaved slice acquisition times, and motion correction. Each participant's functional data were then co-registered to their high resolution anatomical MRI. Data were spatially normalized to an age- and sex-matched pediatric template (age range: 9.9–14.2 yr) created using the TOM8 toolbox (Wilke et al., 2008). Finally, data were spatially smoothed using a Gaussian filter of 5 mm full-width half maximum (FWHM). Additionally, SPM8′s default masking threshold was lowered from 0.8 to 0.7.

*2.3.1.2. First-level analysis.* We generated beta maps for each participant using a general linear model (GLM; Amaro and Barker, 2006) with two predictors based on the experimental events of interest (viz., hits and misses) convolved by the hemodynamic response function as

**Table 1**
Sample characteristics ($N = 51$).

| | FAS/PFAS ($n = 11$[a]) | | HE ($n = 14$) | | Controls ($n = 26$) | | Test statistic | $p$ |
|---|---|---|---|---|---|---|---|---|
| Maternal characteristics | | | | | | | | |
| Age at delivery (years) | 30.8 | (4.0) | 26.0 | (5.2) | 26.4 | (6.1) | 2.97 | 0.061 |
| Level of education (years)[b] | 7.8 | (1.7) | 8.9 | (2.9) | 10.1 | (1.7) | 4.72 | 0.013 |
| Socioeconomic status[c,d] | 11.5 | (2.3) | 21.3 | (8.2) | 26.6 | (6.9) | 19.98 | < 0.001 |
| Food security[e] | | | | | | | | |
| Food secure *n* (% yes) | 2 | (18.2) | 3 | (21.4) | 10 | (38.5) | 2.12 | 0.346 |
| Hunger *n* (% yes) | 8 | (72.7) | 7 | (50.0) | 9 | (34.6) | 4.57 | 0.102 |
| Prenatal alcohol exposure[f] | | | | | | | | |
| AA/day (oz)[g] | 1.3 | (0.8) | 0.9 | (1.0) | 0.0 | (0.0) | 20.10 | <0.001 |
| AA/drinking day (oz)[h] | 4.8 | (2.1) | 3.7 | (3.0) | 0.0 | (0.0) | 34.87 | <0.001 |
| Frequency (days/week)[i] | 1.8 | (0.9) | 1.2 | (1.0) | 0.0 | (0.0) | 31.59 | <0.001 |
| Prenatal smoking (cigarettes/day)[j] | 8.0 | (6.8) | 4.5 | (4.3) | 2.9 | (4.7) | 3.88 | 0.027 |
| Child characteristics | | | | | | | | |
| Gestational age (weeks) | 39.1 | (3.0) | 38.6 | (2.9) | 39.4 | (1.7) | 0.37 | 0.696 |
| Birth weight (g)[k] | 2591.8 | (458.5) | 2765.7 | (503.0) | 3040.6 | (451.7) | 4.03 | 0.024 |
| Age at testing (years)[l] | 12.4 | (1.5) | 10.6 | (0.5) | 11.2 | (1.3) | 7.60 | 0.001 |
| Sex *n* (% male) | 3 | (27.3) | 4 | (28.6) | 8 | (30.8) | 0.05 | 0.974 |
| WISC-IV FSIQ[m] | 65.5 | (10.7) | 76.1 | (17.7) | 77.6 | (12.9) | 3.01 | 0.059 |
| ADHD (% yes) | 2 | (18.2) | 2 | (14.3) | 4 | (15.4) | 0.07 | 0.964 |

*Note.* Unless otherwise stated, values presented are means (standard deviations). FAS = fetal alcohol syndrome; PFAS = partial FAS; HE = heavily exposed non-syndromal; AA = absolute alcohol; WISC-IV = Wechsler Intelligence Scale for Children—Fourth Edition; FSIQ—IV = Full Scale IQ. Test statistics are either $F$ or $\chi^2$ depending on whether the variable was continuous or categorical.

[a] FAS $n = 7$; PFAS $n = 4$.
[b] FAS/PFAS < HE ($p = .04$) and Control ($p = .03$); HE = Control ($p = .83$).
[c] Based on Hollingshead (2011) Inventory.
[d] FAS/PFAS < HE ($p = .001$) and Control ($p = < 0.001$); HE < Control ($p = .02$).
[e] Based on Bickel et al. (2000) guide to measuring household food security.
[f] 1 oz AA/day ≈ 2 standard drinks.
[g] FAS/PFAS = HE ($p = .15$) > Control ($ps < 0.001$).
[h] FAS/PFAS = HE ($p = .14$) > Control ($ps < 0.001$).
[i] FAS/PFAS > HE ($p = .046$) > Control ($ps < 0.001$).
[j] FAS/PFAS = HE ($p = .10$); FAS/PFAS > Control ($p = .008$); HE = Control ($p = .33$).
[k] FAS/PFAS = HE ($p = .36$); FAS/PFAS < Control ($p = .01$); HE < Control ($p = .08$).
[l] FAS/PFAS > HE ($p < .001$) and Control ($p = .006$); HE = Control ($p = .13$).
[m] FAS/PFAS < HE ($p = .07$) and Control ($p = .02$); HE = Control ($p = .76$).

implemented in SPM 8. Additionally, we added each child's movement parameters (displacement, translation and rotation) as nuisance covariates in their first-level model. The contrast of interest was Hit > Miss.

#### 2.3.1.3. Second-level analysis

*2.3.1.3.1. Whole brain voxel-wise analysis.* We performed a whole-brain voxel-wise analysis for the sample as a whole by inserting each participant's Hit > Miss contrast data into a second-level model. The aim of this analysis was to identify clusters showing greater activation for target scenes that were subsequently remembered as 'old' (hits) when compared to target scenes that were later judged as 'new' (misses). After applying a voxel-level threshold of $p$ (family-wise error [FWE] corrected) <0.05, clusters were reported only if they contained >10 contiguous voxels. Each significant cluster was labeled using the Wake Forest University PickAtlas tool (Maldjian et al., 2003, 2004). Anatomical labels generated by PickAtlas that were non-specific (e.g., sub-lobar, extra-nuclear) were reviewed with an experienced neuroanatomist (CMRW), who provided labels with greater descriptive precision. Hereafter, we refer to these regions as the subsequent memory clusters. To assess subsequent memory effects, we extracted beta values for both hit and miss events for each participant for each of the clusters generated by the analysis, using the MarsBaR toolbox (Brett et al., 2002). We then computed differential mean % signal change (Hit – Miss) for each cluster, which represents the effective recruitment of the region predicting subsequent memory formation.

*2.3.1.3.2. Between-group whole brain voxel-wise analysis.* We performed a between-group whole brain voxel-wise analysis to compare patterns of differential activation across FASD diagnostic groups. Between-group contrasts were created using independent-sample $t$-tests. Because of lower power to detect between-group differences, we applied a voxel-level threshold of $p$(uncorrected) < 0.001 and reported clusters with a cluster-level $p$(FWE) < 0.05. Descriptive anatomic labels were assigned to each significant cluster.

### 2.3.2. Additional analyses of effects of exposure on behavioral and neuroimaging data

The data were further analyzed using SPSS (version 23). The distributions of maternal smoking and socioeconomic status, child $d$-prime scores and mean % signal change in several regions (viz., left posterior parahippocampal gyrus, left superior occipital gyrus, left posterior-superior occipital gyrus, right parahippocampal gyrus) each contained one outlier >3 SD above or below the mean. To prevent outliers exerting undue influence on further statistical analysis of these data, these variables were recoded to 1 point above or below the next highest observed value (Winer, 1971).

Nine control variables were examined for inclusion in the statistical analyses: child sex, birth weight, age at testing and IQ; maternal age at delivery, education, socioeconomic status (SES; Hollingshead, 2011), and smoking during pregnancy; and food security (hunger). Any control variable that was related even weakly (at $p < .10$) to a behavioral or neuroimaging outcome was considered as a potential confounder. We planned to re-run any analyses detecting a significant association between PAE and an outcome (at $p < .05$) to include any potential confounders as covariates in an analysis of covariance for the behavioral outcomes and as predictors at the second step in a hierarchical regression analysis for the neuroimaging outcomes. Only one significant endpoint, mean % signal change in the right parahippocampal gyrus, was related to a potential confounder, child sex, and was re-run to adjust statistically for its influence.

One-way analysis of variance (ANOVA) was used to examine

**Table 2**
Between-group differences in behavioral memory performance ($N = 51$).

| | FAS/PFAS ($n = 11$) | | HE ($n = 14$) | | Controls ($n = 26$) | | $F$ | $p$ |
|---|---|---|---|---|---|---|---|---|
| *d*-prime | 0.7 | (0.2) | 0.7 | (0.3) | 0.7 | (0.3) | 0.21 | 0.812 |
| Hit (%) | 43.9 | (9.7) | 51.3 | (11.9) | 42.1 | (8.1) | 4.33[a] | 0.019 |
| False alarm (%) | 29.6 | (10.1) | 35.4 | (10.8) | 27.0 | (10.2) | 2.98[b] | 0.060 |

*Note*. Values presented are means (standard deviations). Percentage data are shown after arcsine transformation. FAS = fetal alcohol syndrome; PFAS = partial FAS; HE = heavily exposed nonsyndromal.
[a] FAS/PFAS < HE ($p = .06$); FAS/PFAS = Control ($p = .60$); HE > Control ($p = .005$).
[b] FAS/PFAS = HE ($p = .17$) and Control ($p = .49$); HE > Control ($p = .02$).

**Table 3**
Whole-brain voxel-wise comparison showing differential subsequent memory activation ($N = 51$).

| Hit > Miss voxel-level $p$(FWE) < 0.05 | | | | | | | |
|---|---|---|---|---|---|---|---|
| | | MNI Coordinates | | | | | |
| Region | BA | x | y | z | Peak $t$ value | Cluster size (No. voxels) | Cluster-level $p$(unc) value |
| Parietal | | | | | | | |
| L Intraparietal sulcus | – | −22 | −66 | 54 | 6.97 | 36 | < 0.001 |
| *L Intraparietal sulcus* | – | −22 | −60 | 46 | 5.76 | | |
| R Intraparietal sulcus (medial branch) | – | 20 | −64 | 52 | 6.45 | 11 | 0.008 |
| Occipital | | | | | | | |
| R Middle occipital gyrus (lateral surface, occipital) | 39 | 44 | −78 | 26 | 7.95 | 305 | < 0.001 |
| *R Superior occipital gyrus (occipital)* | – | 32 | −82 | 26 | 7.64 | | |
| *R Middle occipital gyrus (occipital)* | – | 32 | −86 | 10 | 7.02 | | |
| R Posterior inferior temporal gyrus | – | 52 | −62 | −12 | 7.93 | 51 | < 0.001 |
| *R Posterior-superior inferior temporal gyrus* | – | 42 | −62 | −8 | 6.08 | | |
| L Posterior superior occipital gyrus | – | −42 | −84 | 24 | 7.91 | 57 | < 0.001 |
| L Inferior occipital gyrus | – | −48 | −60 | −8 | 7.47 | 142 | < 0.001 |
| *L Posterior-superior inferior temporal gyrus* | – | −48 | −52 | −14 | 6.67 | | |
| *L Inferior occipital gyrus* | – | −48 | −72 | −4 | 6.00 | | |
| R Posterior-superior inferior temporal gyrus (occipital) | – | 52 | −52 | −10 | 6.44 | 39 | < 0.001 |
| L Superior occipital gyrus (lateral surface) | 19 | −30 | −84 | 28 | 6.37 | 45 | < 0.001 |
| Limbic | | | | | | | |
| L Posterior parahippocampal gyrus | – | −20 | −36 | −12 | 8.43 | 378 | < 0.001 |
| *L Parahippocampal gyrus* | 36 | −26 | −30 | −20 | 8.27 | | |
| *L Parahippocampal gyrus* | 37 | −30 | −40 | −14 | 7.77 | | |
| R Parahippocampal gyrus | 37 | 32 | −38 | −12 | 7.78 | 212 | < 0.001 |
| *R Parahippocampal gyrus* | – | 24 | −36 | −14 | 7.76 | | |
| *R Fusiform gyrus (occipital-temporal junction)* | 37 | 34 | −48 | −18 | 7.45 | | |
| Hippocampus | | | | | | | |
| R Hippocampus, tail | – | 18 | −34 | −2 | 6.12 | 11 | 0.008 |

*Note.* Significant clusters were reported only if they contained > 10 contiguous voxels. In cases where significant submaxima clusters were identified, details are provided in italics under maxima. FWE = family-wise error corrected; MNI = Montréal Neurological Institute; BA = Brodmann Area; Unc = uncorrected; L = left; R = right.

between-group differences (FAS/PFAS, nonsyndromal HE, Controls) in performance on the post-scan recognition task. *d*-Prime was used as the principal behavioral outcome as it is a measure of recognition accuracy that corrects for response bias, random guessing and possible fatigue effects. *d*-prime was calculated as *hit rate - false alarm rate,* where the hit and false alarm rates have been transformed to z-scores. Hit and false alarm rates were also examined using ANOVA after being subjected to arcsine transformation to adjust for heteroscedasticity typically found in proportional data. Where significant between-group differences were found, we ran least-significant difference (LSD) *post-hoc* tests.

We also conducted an exploratory analysis to assess the degree to which level of PAE in the FAS/PFAS and HE groups predicted changes in activation levels in the subsequent memory clusters. Pearson correlation analysis was used to examine associations between two continuous measures of PAE (oz AA/day and oz AA/drinking day) and mean % signal change (Hit – Miss) in the subsequent memory clusters within each of the alcohol-exposed groups.

## 3. Results

### 3.1. Sample characteristics

Mothers of children in the FAS/PFAS group were more economically disadvantaged than those in the HE and Control groups and had completed fewer years of formal education and smoked more during pregnancy than Controls (Table 1). Mothers of the HE children were more economically disadvantaged than those of the Controls. Although mothers in the FAS/PFAS and HE groups did not differ in terms of alcohol consumption averaged across pregnancy (AA/day) or average dose/occasion (AA/drinking day), those in the FAS/PFAS group drank twice as frequently (~2 days/week) than those in the HE group (~1 day/week). All but one of the Control mothers abstained from using alcohol during pregnancy; that mother reported drinking four drinks on one occasion early in the pregnancy. None of the mothers reported using cocaine during pregnancy. Five (1 FAS/PFAS, 3 HE, and 1 Control) reported using marijuana ($M = 2.1$ times/month), and three (1 FAS/PFAS and 2 HE) reported using methaqualone ($M = 1.3$ times/month). Because prenatal drug exposure was too rare for statistical adjustment, we re-ran any analyses detecting an association between PAE and an

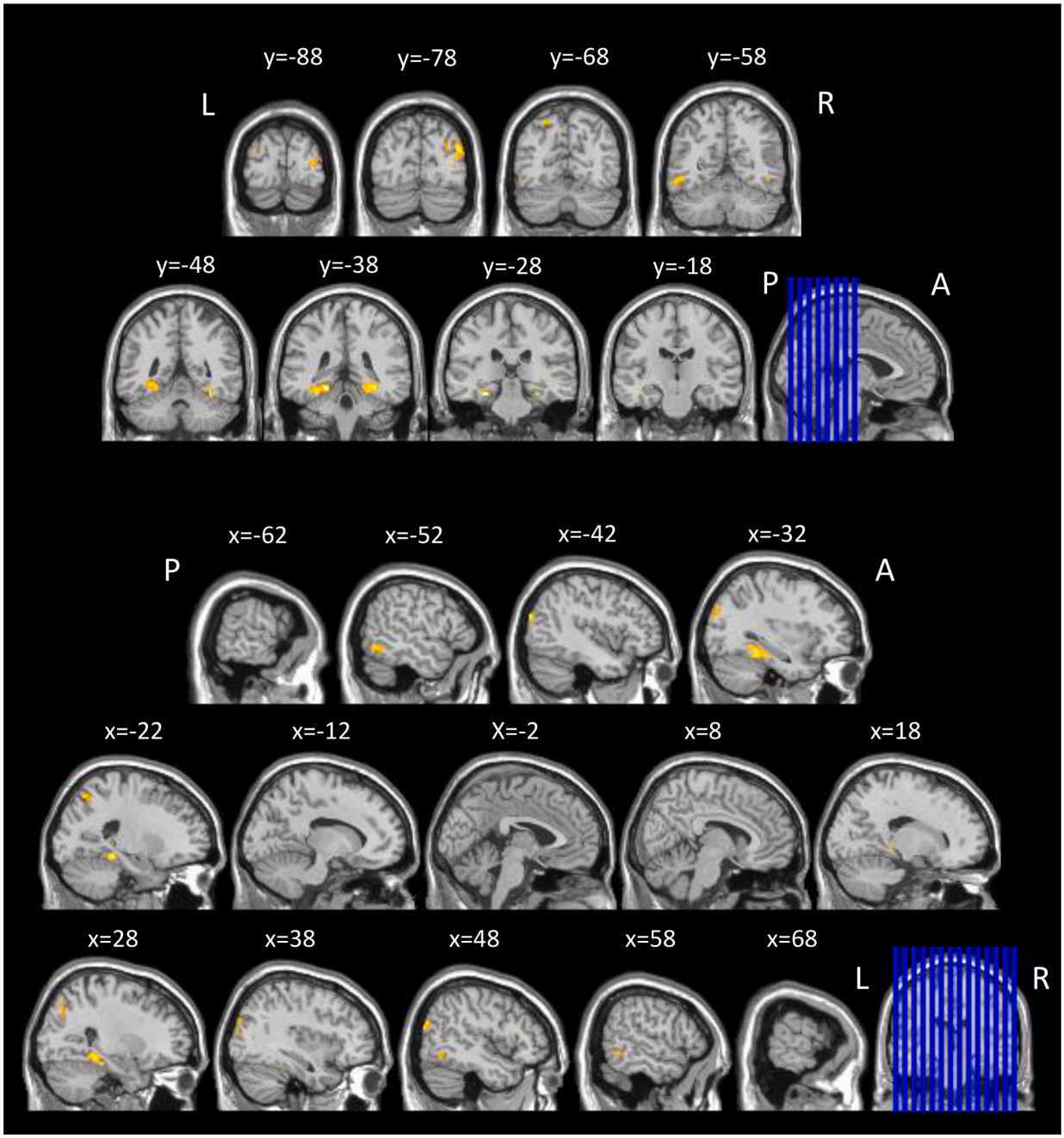


**Fig 1.** Whole-brain composite activations for Hits > Misses. SPM activation map overlaid on T1 single-subject template, thresholded at $p$(FWE) < 0.05, and shown for selected (a) coronal and (b) sagittal slices. L = left; R = right; A = anterior; P = posterior. The blue lines on the sagittal and coronal images in (a) and (b), respectively, indicate the positions of the slices shown. Slice positions are given in MNI coordinates. (For interpretation of the references to colour in this figure legend, the reader is referred to the web version of this article.)

observed outcome measure omitting the children with either marijuana or methaqualone exposure. All effects remained essentially unchanged. Five children (3 FAS/PFAS, 1 HE and 1 Control) were born preterm (i.e., gestational age < 37 weeks; median = 35.3). Birth weight was lower in children in the FAS/PFAS group than in children in the Control group. Children in the FAS/PFAS group were older than those in other two groups and had lower IQ scores than Controls.

### 3.2. Behavioral data: Performance on the post-scan recognition task

Among the 51 children in the final study sample, *d*-prime ranged from 0.3 to 2.0 (median = 0.7). The groups did not differ in recognition accuracy measured by *d*-prime (Table 2). Correct hit rate averaged 49.8% across the sample as a whole prior to the arcsine transformation. Although overall accuracy (*d*-prime) did not differ between groups, there were small but significant group differences in behavioral response patterns. The response pattern of children in the FAS/PFAS group was similar to that of Controls, but the HE children had more correct hits and more false alarms than Controls.

### 3.3. Neuroimaging data: Memory encoding activation

#### 3.3.1. Whole brain voxel-wise analysis for the sample as a whole

In the whole brain analysis for the hit > miss contrast for sample as a whole, 11 clusters (excluding sub-maxima clusters) showed activation increases for target scenes subsequently remembered as 'old' (hits) when

compared to those later judged as 'new' (misses; Table 3, Fig. 1). This pattern of activation included a large band in the occipital cortex, bilaterally, with extension dorsally to the bilateral intraparietal sulci and ventrally to the bilateral parahippocampal gyri and right hippocampal formation.

#### 3.3.2. Between-group whole brain voxel-wise analyses

Voxel-wise between-group comparisons revealed greater subsequent memory activation in the FAS/PFAS group compared to Controls, in the left postcentral sulcus, and compared to HE, in the left precentral gyrus, left paracentral lobule and right posterior-superior temporal sulcus (Table 4; Figs. 2 and 3, respectively).

#### 3.3.3. Correlations between continuous measures of PAE and activation levels in the subsequent memory clusters identified in Table 3

Within the FAS/PFAS group, one continuous measure of PAE, AA/drinking day, was related to mean % signal change in 3 subsequent memory clusters, all of which were located in the medial temporal lobe (Table 5, Fig. 4). Higher levels of AA/drinking day were associated with lower levels of activation in the left and right parahippocampal gyri and with greater activation in right hippocampus. Mean % signal change in the right parahippocampal gyrus was associated with child sex, which was, therefore, considered a potential confounder of the effect of AA/drinking day; however, the significant alcohol effect persisted after controlling for child sex, with a standardized regression coefficient for AA/drinking day of $\beta = -0.62$, $p < .05$.

## 4. Discussion

The primary aim of this study was to examine neural activation predicting successful memory formation in children with heavy PAE. We assessed activation using an event-related fMRI task for the subsequent memory paradigm adapted by Ofen and colleagues (Ofen et al., 2007; Tang et al., 2018). Analyses of the behavioral data did not detect significant between-group differences in recognition accuracy. Analyses of the neuroimaging data indicated that, across the entire sample, children recruited extensive bilateral networks, including the right hippocampal formation, occipital cortex and posterior parietal cortex, during successful memory formation. This pattern of subsequent memory effects is consistent with previous fMRI studies of typically developing children (Chai et al., 2010). In addition to activating this network, children with a diagnosis of FAS or PFAS also showed greater subsequent memory activations in the right posterior superior temporal sulcus, left precentral gyrus and left paracentral lobule than HE children and in the left postcentral sulcus than Control children. Given the absence of between-group differences in recognition accuracy, these data suggest that during encoding the children with FAS and PFAS recruited more extensive neural resources to successfully form memories of the target stimuli. To the best of our knowledge, this is the first study to demonstrate impairment at the level of brain function supporting subsequent memory deficits in FASD.

The behavioral performance of our participants was consistent with performance accuracy levels reported in studies of healthy children and young adults. On the same fMRI subsequent memory task used in this study, Ofen et al. (2007) reported a hit rate of 51% and a correct rejection rate of 79% for their sample ($N = 49$; age range: 8–24 yr). Tang et al (2018) reported similar hit and correct rejection rates (57% and 74%, respectively) for their sample ($N = 83$; age range: 8–25 yr). Given that the age range of our sample was narrower, it is impressive that our hit rates were so similar (viz., hit rate of 49.8% and correct rejection rate of 73.5%). Moreover, the absence of between-group differences in recognition accuracy indicates that the alcohol-exposed participants had little difficulty understanding the task instructions.

The subsequent memory effects observed here validate the use of this event-related fMRI task in this pediatric clinical sample. The regions that showed greater activation for target scenes that were subsequently remembered as 'old' (hits) when compared to target scenes that were later judged as 'new' (misses) are consistent with those reported in adult samples (Kim, 2011) and in typically-developing pediatric samples (Chai et al., 2010; Maril et al., 2011; Shing et al., 2016). The activation patterns we observed are also consistent with those suggested by Kim (2011), reflecting broad functional units associated with three processes integral to effective memory encoding: (1) content processing (e.g., posterior parahippocampal gyrus activation during visual scene processing; Epstein and Kanwisher, 1998); (2) information storage (e.g., MTL and hippocampal formation during the binding of content and

**Table 4**
Between-group whole-brain voxel-wise comparison showing differential subsequent memory activation ($N = 51$).

| Hit > Miss, voxel-level $p$(unc) < 0.001 | | | | | | | |
|---|---|---|---|---|---|---|---|
| Region | BA | MNI Coordinates x | y | z | Peak $t$ value | Cluster size (No. Voxels) | Cluster-level $p$(FWE) value |
| Control > FAS/PFAS | | | No significant differences | | | | |
| Control > HE | | | No significant differences | | | | |
| HE > Control | | | No significant differences | | | | |
| HE > FAS/PFAS | | | No significant differences | | | | |
| FAS/PFAS > Control | | | | | | | |
| Frontal | | | | | | | |
| L Postcentral sulcus (extending into paracentral white matter) | – | −14 | −32 | 68 | 5.14 | 208 | < 0.001 |
| *L Paracentral lobule* | – | −2 | −36 | 64 | 3.89 | | |
| *R Paracentral lobule* | – | 4 | −40 | 52 | 3.85 | | |
| FAS/PFAS > HE | | | | | | | |
| Frontal | | | | | | | |
| L Precentral gyrus | – | −14 | −32 | 68 | 4.77 | 94 | 0.028 |
| *L Precentral gyrus* | 4 | −22 | −28 | 66 | 4.01 | | |
| *L Precentral gyrus* | – | −28 | −28 | 54 | 3.90 | | |
| L Paracentral lobule | 5 | −12 | −38 | 52 | 4.70 | 88 | 0.037 |
| *L Precuneus (Parietal)* | 7 | −2 | −42 | 48 | 3.60 | | |
| Temporal | | | | | | | |
| R Posterior superior temporal sulcus (close proximity to occipital-temporal junction) | – | 40 | −64 | 20 | 4.43 | 82 | 0.049 |
| *R Posterior superior temporal sulcus* | – | 36 | −54 | 24 | 3.97 | | |

*Note.* Significant clusters were reported only if they contained > 10 contiguous voxels. In cases where significant submaxima clusters were identified, details are provided in italics under maxima. Unc = uncorrected; MNI = Montréal Neurological Institute; BA = Brodmann Area; FWE = family-wise error corrected; FAS = fetal alcohol syndrome; PFAS = partial FAS; HE = heavily exposed nonsyndromal; L = left; R = right.

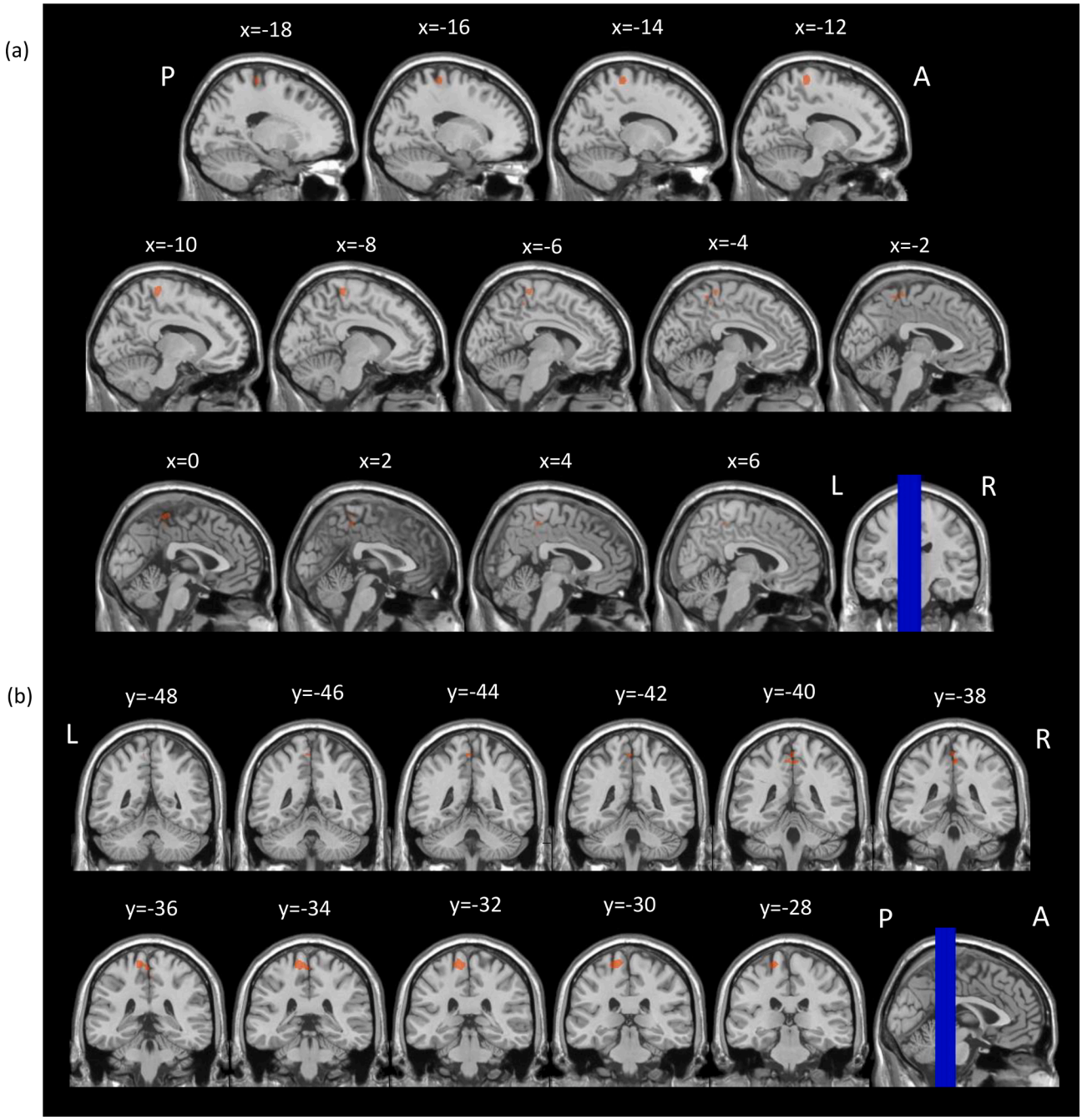


**Fig. 2.** Regions where children with FAS/PFAS showed greater subsequent memory activation than Control children. SPM activation maps overlaid on T1 single-subject template, thresholded at a voxel-level $p$(unc) < 0.001 and cluster-level $p$(FWE) < 0.05. Images shown are for selected (a) sagittal and (b) coronal slices. L = left; R = right; A = anterior; P = posterior. The blue lines on the coronal and sagittal images in (a) and (b), respectively, indicate the positions of the slices shown. Slice positions are given in MNI coordinates. (For interpretation of the references to colour in this figure legend, the reader is referred to the web version of this article.)

memory representation; Henke et al., 1997); and (3) attention (e.g., a frontoparietal network that recruits primary motor cortex and posterior parietal cortex during tasks assessing visual attention; Corbetta et al., 2002; 2008).

During successful memory formation, children in the FAS/PFAS group showed greater subsequent memory activation in the left post-central sulcus relative to Controls. This region forms a part of the posterior parietal attentional and perceptual networks supporting visual scene processing (Donner et al., 2000). This finding is consistent with Sowell et al.'s (2007) report of more extensive neural recruitment during memory processing in participants with heavy PAE compared to Controls. Compared to HE participants, those with FAS/PFAS showed greater subsequent memory activation in the left precentral gyrus, left paracentral lobule, and right posterior-superior temporal sulcus. These regions have been characterized as contributing to the frontoparietal attention network described above (Corbetta et al., 2002; 2008), with the observed pattern of activation suggesting compensatory attentional processing during successful memory formation. These data are also consistent with (a) those reported by other fMRI studies of PAE, in which exposed participants showed greater recruitment of parietal visual attention networks on spatial working memory and number processing tasks (Malisza et al., 2012; Woods et al., 2015), and (b) the general

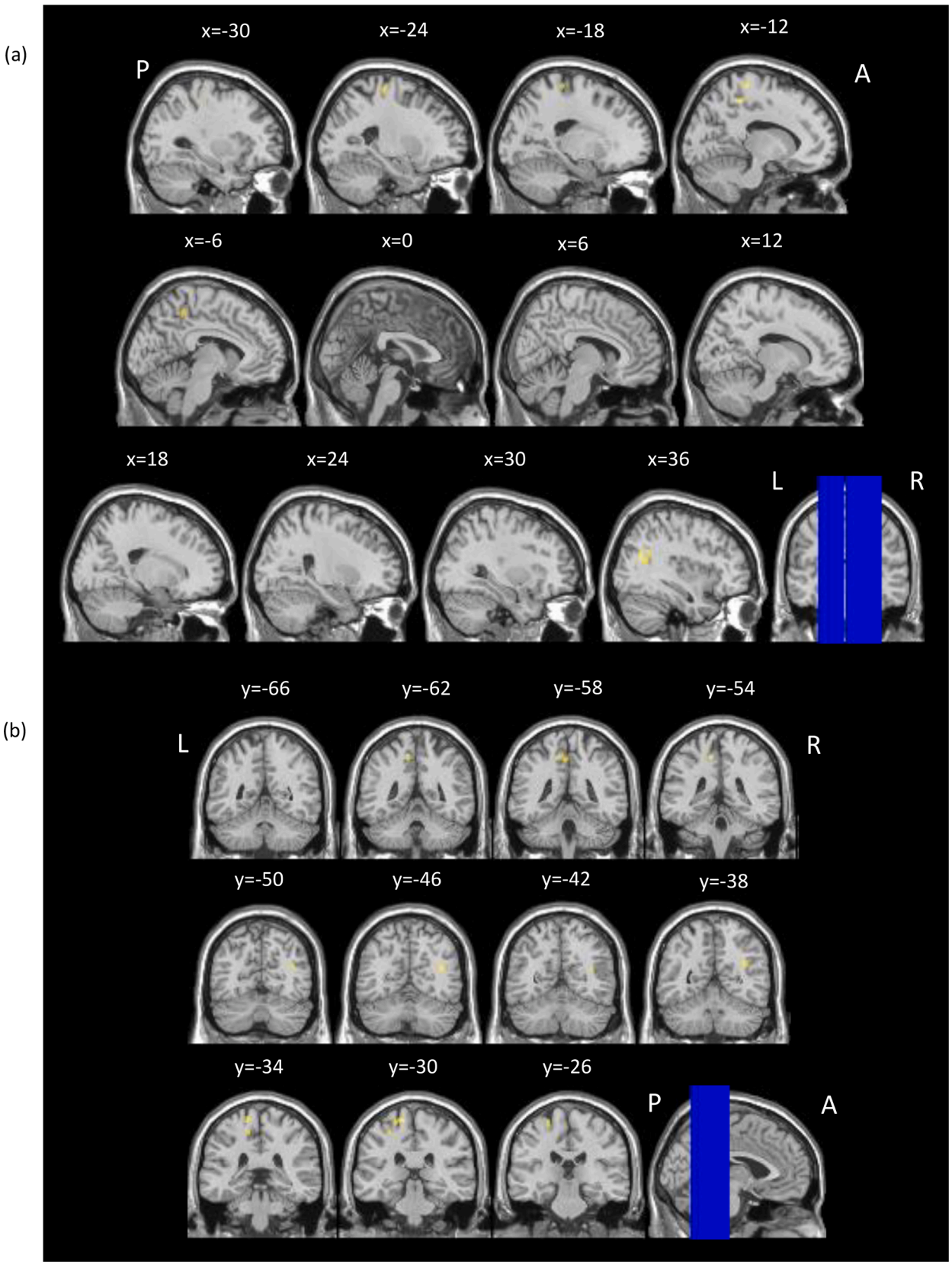


**Fig. 3.** Regions where children with FAS/PFAS showed greater subsequent memory activation than HE children. SPM activation maps overlaid on T1 single-subject template, thresholded at a voxel-level $p$(unc) $< 0.001$ and cluster level $p$(FWE) $< 0.05$. Images are shown for selected (a) sagittal and (b) coronal slices. L = left; R = right; A = anterior; P = posterior. The blue lines on the coronal and sagittal images in (a) and (b), respectively, indicate the positions of the slices shown. Slice positions are given in MNI coordinates. (For interpretation of the references to colour in this figure legend, the reader is referred to the web version of this article.)

**Table 5**
Relation of continuous prenatal alcohol exposure to magnitude of activation in subsequent memory clusters (Hit > Miss).

| | FAS/PFAS ($n = 11$[a]) | | HE ($n = 14$) | |
|---|---|---|---|---|
| | AA/day | AA/drinking day | AA/day | AA/drinking day |
| Region | *r* | *r* | *r* | *r* |
| Parietal | | | | |
| L Intraparietal sulcus | 0.39 | 0.24 | −0.11 | −0.23 |
| R Intraparietal sulcus (medial branch) | 0.50 | −0.03 | −0.04 | 0.01 |
| Occipital | | | | |
| R Middle occipital gyrus (lateral surface, occipital) | −0.34 | −0.30 | −0.14 | −0.02 |
| R Posterior inferior temporal gyrus | −0.29 | −0.42 | −0.19 | −0.03 |
| L Posterior superior occipital gyrus | −0.27 | −0.17 | 0.13 | −0.04 |
| L Inferior occipital gyrus | −0.32 | −0.48 | −0.15 | 0.01 |
| R posterior-superior inferior temporal gyrus (occipital) | −0.06 | −0.27 | 0.16 | 0.21 |
| L Superior occipital gyrus (lateral surface) | −0.15 | −0.45 | 0.07 | 0.22 |
| Limbic | | | | |
| L Posterior parahippocampal gyrus | −0.15 | **−.67**[b] | −0.13 | −0.03 |
| R Parahippocampal gyrus | −0.04 | **−.62**[c] | −0.08 | −0.13 |
| Hippocampus | | | | |
| R Hippocampus, tail | 0.22 | **.66**[d] | −0.10 | 0.10 |

*Note.* Values are Pearson correlation coefficients (*r*). All significant effects remained significant at $p < .05$ after adjustment for potential confounders. FAS = fetal alcohol syndrome; PFAS = partial FAS; HE = heavily exposed nonsyndromal; AA = absolute alcohol; L = left; R = right.
[a] FAS n = 7; PFAS n = 4.
[b] $p = .03$.
[c] $p = .04$.
[d] $p = .03$.

pattern of more diffuse fMRI activation in children with FAS/PFAS (Diwadkar et al., 2013; Fryer et al., 2007a; Meintjes et al., 2010), which is suggestive of compensatory activation mediating effective behavioral task completion.

In the FAS/PFAS group, exploratory analyses showed a link between level of exposure and differential activation in three important subsequent memory clusters. Specifically, average alcohol dose/drinking day was associated with decreased activation in the bilateral parahippocampal gyri and increased activation in the right hippocampus. Within this group, the latter pattern of activation may act as a compensatory mechanism for the former. The parahippocampal gyri form a part of the ventral visual processing stream that is implicated in the initial processing and integration of visual-spatial information into long-term memory (Epstein and Kanwisher, 1998, Henson and Gagnepain, 2010). The hippocampal formation plays an integral role in the acquisition and consolidation of novel information into long-term memory (Eichenbaum, 2003; Winocur et al., 2010). Because these analyses were exploratory, these findings warrant replication in a future study.

Taken together with the between-group differences, the exploratory analyses suggest PAE-related functional impairment in regions mediating visual attention and integration of perceptual information during memory encoding and in regions involved in memory acquisition and consolidation. Although IQ scores were lower in the FAS/PFAS group than the Controls, IQ was not correlated with activation levels in any of the regions affected by PAE, suggesting that the observed effects of PAE are specific to memory formation and not attributable to generalized intellectual disability in children with FAS and PFAS.

### 4.1. Limitations and future directions

The sample size for both the FAS/PFAS and HE groups was small but similar to (if not slightly larger than) previous neuroimaging studies in children with heavy PAE (e.g., heavy PAE $n = 11$, Sowell et al., 2007;

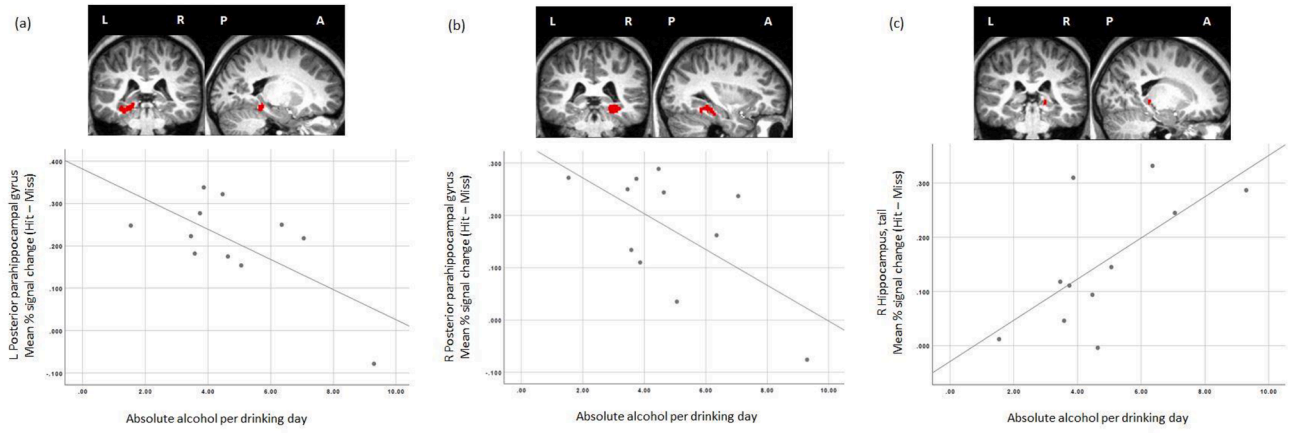


**Fig.4.** Scatterplots indicating the association between mean % change (Hit – Miss) and average absolute alcohol per drinking day in three subsequent memory clusters: (a) left parahippocampal gyrus (MNI coordinates: −20, −36, −12), (b) right parahippocampal gyrus (MNI coordinates: 32, −38, −12), and (c) right hippocampus, tail (MNI coordinates: 18, −34, −2). Clusters overlaid on a single Control participant's T1 weighted structural image. L = left; R = right; P = posterior; A = anterior.

FAS/PFAS $n = 17$, nonsyndromal HE $n = 13$, Diwadkar et al., 2013). Movement during neuroimaging data acquisition was the primary constraining factor on sample size due to the need to exclude participants whose movement exceeded acceptable thresholds. However, it is a relative strength of the current study that the participants included in the analyses showed no more than minimal movement artifact. The smaller sample sizes in the alcohol-exposed groups resulted in reduced power to detect voxel-wise between-group differences in subsequent memory activation at a voxel-level threshold of $p(\text{FWE}) < 0.05$. These findings, therefore, warrant further investigation in a larger sample.

PAE also has extensive effects on brain morphology, which may affect functional activation patterns (Coles and Li, 2011; Meintjes et al., 2014; Fan et al., 2016). For example, Li et al. (2008) found that the location of functional impairment associated with heavy PAE in the occipital-temporal cortex was consistent with volumetric reductions in white and gray matter in this region. Thus, underlying structural abnormalities may mediate the effect of PAE on functional activation in a given region. Given that exposure-related structural impairments have been documented in several of the regions recruited during successful memory formation in this study (for a review, see Moore et al., 2014), it would be of interest to examine structural and functional data simultaneously in regions demonstrating subsequent memory effects.

Co-morbid diagnoses of ADHD and behavioral symptoms similar to those observed in ADHD are frequently reported in children with PAE (Aronson et al., 1997; Coles, 2001; Fryer et al., 2007b; Mick et al., 2002). However, the etiology and neuropsychological presentation of children with both PAE and ADHD differs from those in children with idiopathic ADHD (Crocker et al., 2011; Jacobson et al., 2011; Kingdon et al., 2016). Krauel et al. (2007) demonstrated that, during encoding, adolescents with ADHD activate additional regions in the superior parietal lobe and precuneus, a pattern suggestive of compensatory activation of attentional resources. Although we also found compensatory activation patterns in the FAS/PFAS group in this study, they occurred in somewhat different regions (e.g., greater hippocampal recruitment). These patterns of compensatory activation suggest that it may be possible to use the subsequent memory paradigm to differentiate between the encoding difficulties observed in FASD and ADHD in future studies with larger sample sizes.

### 4.2. Conclusions

This is the first study to examine patterns of neural activation predictive of successful memory formation in children with FASD and to report subsequent memory effects in a pediatric PAE-affected sample. Unlike the previous fMRI study investigating this topic (Sowell et al., 2007), which treated learning (encoding) and memory (recall/retrieval) impairment as representative of a single deficit, the current study design allowed us to examine PAE effects on activation patterns specifically during the encoding phase in successful memory formation. Within the FAS/PFAS group, we observed a reduction in activation in the parahippocampal gyri that appears to be compensated for by the recruitment of additional neural regions outside of the subsequent memory network identified for the sample as a whole, as well as increased activation in the hippocampus. This study provides a novel contribution to the literature by validating the subsequent memory paradigm for use in this clinical population and by demonstrating that children with FAS and PFAS recruit compensatory attentional and other neural resources to support successful memory formation.

## Author contributions

CEL conducted this study as part of her doctoral dissertation. She reviewed the literature, contributed to the conceptualization and design of the study, administered neurobehavioral and neuroimaging assessments, conducted the data analysis and interpretation of the findings, and wrote up the paper for publication.

KGFT supervised CEL's dissertation, contributed to the data analysis and interpretation of the findings, and reviewed the manuscript

NO provided the fMRI paradigm, contributed to the interpretation of the findings, and reviewed the manuscript

CMRW, an expert neuroanatomist, advised CEL on the interpretation of the neuroimaging data

FR contributed to the data analysis and interpretation of the findings and reviewed the manuscript

NML administered neurobehavioral and neuroimaging assessments and contributed to the analysis of the neuroimaging data by constructing the heat maps

CDM collaborated on the longitudinal Cape Town FASD study, supervised the behavioral research staff and administered the maternal interviews, including collection of sociodemographic information and alcohol, smoking and drug ascertainment

EM collaborated on the design of the neuroimaging study, contributed to the analysis and interpretation of the neuroimaging data, and the write-up of the paper

SWJ and JLJ designed and recruited the original Cape Town FASD prospective longitudinal study and subsequent follow-up maternal and child assessments, including the alcohol and drug exposure ascertainment and the neuropsychological and neuroimaging assessments. They contributed to the conceptualization of CEL's doctoral study, data analysis and interpretation and write-up of the paper

## Declaration of Competing Interest

The authors declare that they have no known competing financial interests or personal relationships that could have appeared to influence the work reported in this paper.

## *Acknowledgments*

**Funding sources**:

The Cape Town Longitudinal Study is supported by grants from NIH/National Institute on Alcohol Abuse and Alcoholism (NIAAA) R01-AA016781, two supplements to RO1-AA09524; U01-AA014790 and U24AA014815; NIH Office of Research on Minority Health; and Lycaki-Young Fund, from the State of Michigan. Further financial support for this study was provided by the National Research Foundation (NRF) and University of Cape Town (UCT).

We thank Denis L. Viljoen, M.D., for his collaboration on the recruitment of the Cape Town Longitudinal Cohort; our University of Cape Town research staff, Maggie September, Beverley Arendse, Patricia Solomons, Landi Meiring, for their contributions to subject recruitment, transportation, and data collection, and our Wayne State University (WSU) research staff, Neil Dodge, Ph.D., and Renee Sun, for assistance with data management and analysis; Keri Woods, Ph.D., for her help formatting the neuroimaging task for use in this study; and Vaibhav Diwadkar, Ph.D., for the neuroimaging training that he provided at WSU. We also thank H. Eugene Hoyme, M.D. and Luther K. Robinson, M.D., who conducted the dysmorphology examinations at our 2005 FASD diagnostic clinic. We also wish to express our appreciation to the mothers and children who have participated in this longitudinal study.

## References

Amaro, E., Barker, G.J., 2006. Study design in fMRI: Basic principles. Brain Cognit. 60, 220–232.

American Psychiatric Association, 1994. Diagnostic and Statistical Manual of Mental Disorders. Washington, DC.

Aronson, M., Hagberg, B., Gillberg, C., 1997. Attention deficits and autistic spectrum problems in children exposed to alcohol during gestation: A follow-up study. Dev. Med. Child. Neurol. 39, 583–587.

Bearer, C.F., Jacobson, J.L., Jacobson, S.W., Barr, D., Croxford, J.A., Molteno, C.D., Viljoen, D.L., Marais, A.-S., Chiodo, L.M., Cwik, A.S., 2003. Validation of a new biomarker of fetal exposure to alcohol. J. Pediatr. 143, 463–469.

Bickel, G., Nord, M., Price, C., Hamilton, W., Cook, J. 2000. Guide to measuring household food security. USDA. Food and Nutrition Service.
Bowman, R.S., Stein, L.I., Newton, J.R., 1975. Measurement and interpretation of drinking behaviour. Q. J. Stud. Alcohol 36, 1154–1172.
Brett, M., Anton, J.-L., Valabregue, R., Poline, J.-B., 2002. Region of interest analysis using an SPM toolbox. NeuroImage 16, S497.
Brewer, J.B., Zhao, Z., Desmond, J.E., Glover, G.H., Gabrieli, J.D.E., 1998. Making memories: brain activity that predicts how well visual experience will be remembered. Science 281, 1185–1187.
Chai, X.J., Ofen, N., Jacobs, L.F., Gabrieli, J.D.E., 2010. Scene complexity: Influence on perception, memory, and development in the medial temporal lobe. Front. Hum. Neurosci. 4, 1–10.
Chai, X.J., Ofen, N., Gabrieli, J.D., Whitfield-Gabrieli, S., 2014. Development of deactivation of the default-mode network during episodic memory formation. Neuroimage. 84, 932–938.
Coles, C.D., 2001. Fetal alcohol exposure and attention: Moving beyond ADHD. Alcohol Res. Health. 25, 199–203.
Coles, C.D., Li, Z., 2011. Functional neuroimaging in the examination of effects of prenatal alcohol exposure. Neuropsychol. Rev. 21, 119–132.
Corbetta, M., Kincade, J.M., Shulman, G.L., 2002. Neural systems for visual orienting and their relationships to spatial working memory. J. Cognitive Neurosci. 14, 508–523.
Corbetta, M., Patel, G., Shulman, G.L., 2008. Review the reorienting system of the human brain: From environment to theory of mind. Neuron 58, 306–324.
Crocker, N., Vaurio, L., Riley, E.P., Mattson, S.N., 2011. Comparison of verbal learning and memory in children with heavy prenatal alcohol exposure or attention-deficit/hyperactivity disorder. Alcohol Clin. Exp. Res. 35, 1–8.
Croxford, J., Viljoen, D., 1999. Alcohol consumption by pregnant women in the Western Cape. S. Afr. Med. J. 89, 962–965.
Diwadkar, V.A., Meintjes, E.M., Goradia, D., Dodge, N.C., Warton, C., Molteno, C.D., Jacobson, S.W., Jacobson, J.L., 2013. Differences in cortico-striatal-cerebellar activation during working memory in syndromal and nonsyndromal children with prenatal alcohol exposure. Hum. Brain Mapp. 34, 1931–1945.
Donner, T., Kettermann, A., Diesch, E., Ostendorf, F., Villringer, A., Brandt, S.A., 2000. Involvement of the human frontal eye field and multiple parietal areas in covert visual selection during conjunction search. Eur. J. of Neurosci. 12, 3407–3414.
du Plooy, C.P., Malcolm-Smith, S., Adnams, C.M., Stein, D.J., Donald, K.A., 2016. The effects of prenatal alcohol exposure on episodic memory functioning: A systematic review. Arch. Clin. Neuropsych. 31, 710–726.
Eichenbaum, H., 2003. The hippocampus, episodic memory, declarative memory, spatial memory…where does it all come together? Int. Congr. Ser. 1250, 235–244.
Epstein, R., Kanwisher, N., 1998. A cortical representation of the local visual environment. Nature 392, 598–601.
Fan, J., Jacobson, S.W., Taylor, P.A., Molteno, C.D., Dodge, N.C., Stanton, M.E., Jacobson, J.L., Meintjes, E.M., 2016. White matter deficits mediate effects of prenatal alcohol exposure on cognitive development in childhood. Hum. Brain Map. 37, 2943–2958.
Fryer, S.L., McGee, C.L., Matt, G.E., Riley, E.P., Mattson, S.N., 2007a. Evaluation of psychopathological conditions in children with heavy prenatal alcohol exposure. Pediatrics 119, e733–e741.
Fryer, S.L., Tapert, S.F., Mattson, S.N., Paulus, M.P., Spadoni, A.D., Riley, E.P., 2007b. Prenatal alcohol exposure affects frontal-striatal BOLD response during inhibitory control. Alcohol Clin. Exp. Res. 31, 1415–1424.
Gross, L.A., Moore, E.M., Wozniak, J.R., Coles, C.D., Kable, J.A., Sowell, E.R., Jones, K.L., Riley, E.P., Mattson, S.N., CIFASD, 2017. Neural correlates of verbal memory in youth with heavy prenatal alcohol exposure. Brain Imaging Behav. https://doi.org/10.1007/s11682-017-9739-2.
Hallowell, L.M., Stewart, S.E., de Amorim E Silva, C.T., Ditchfield, M.R., 2008. Reviewing the process of preparing children for MRI. Pediatr. Radiol. 38, 271–279.
Henke, K., Buck, A., Weber, B., Wieser, H.G., 1997. Human hippocampus establishes associations in memory. Hippocampus 7, 249–256.
Henson, R.N., Gagnepain, P., 2010. Predictive, interactive multiple memory systems. Hippocampus 20, 1315–1326.
Hollingshead, A.B., 2011. Four factor index of socioeconomic status. Yale J. Sociol. 8, 21–52.
Hoyme, H.E., May, P.A., Kalberg, W.O., Kodituwakku, P., Gossage, J.P., Trujillo, P.M., Buckley, D.G., Miller, J.H., Aragon, A.S., Khaole, N., Viljoen, D.L., Jones, K.L., Robinson, L.K., 2005. A practical clinical approach to diagnosis of fetal alcohol spectrum disorders: clarification of the 1996 Institute of Medicine criteria. Pediatrics 115, 39–47.
Jacobson, J.L., Dodge, N.C., Burden, M.J., Klorman, R., Jacobson, S.W., 2011. Number processing in adolescents with prenatal alcohol exposure and ADHD: differences in the neurobehavioral phenotype. Alcohol Clin. Exp. Res. 35, 431–442.
Jacobson, S.W., Chiodo, L.M., Jacobson, J.L., Sokol, R.J., 2002. Validity of maternal report of alcohol, cocaine, and smoking during pregnancy in relation to infant neurobehavioral outcome. Pediatrics 109, 815–825.
Jacobson, S.W., Jacobson, J.L., Molteno, C.D., Warton, C.M.R., Wintermark, P., Hoyme, H.E., De Jong, G., Taylor, P., Warton, F., Lindinger, N.M., Carter, R.C., Dodge, N.C., Grant, E., Warfield, S.K., Zöllei, L., van der Kouwe, A.J.W., Meintjes, E. M., 2017. Heavy prenatal alcohol exposure is related to smaller corpus callosum in newborn MRI scans. Alcohol Clin. Exp. Res. 41, 965–975.
Jacobson, S.W., Stanton, M.E., Molteno, C.D., Burden, M.J., Fuller, D.S., Hoyme, H.E., Robinson, L.K., Khaole, N., Jacobson, J.L., 2008. Impaired eyeblink conditioning in children with fetal alcohol syndrome. Alcohol Clin. Exp. Res. 32, 365–372.
Kaemingk, K.L., Mulvaney, S., Halverson, P.T., 2003. Learning following prenatal alcohol exposure: performance on verbal and visual multitrial tasks. Arch. Clin. Neuropsych. 18, 33–47.
Kim, H., 2011. Neural activity that predicts subsequent memory and forgetting: a meta-analysis of 74 fMRI studies. NeuroImage 54, 2446–2461.
Kingdon, D., Cardoso, C., McGrath, J.J., 2016. Executive function deficits in fetal alcohol spectrum disorders and attention-deficit/hyperactivity disorder – A meta-analysis. J. Child Psychol. Psyc. 57, 116–131.
Kodali, V.N., Jacobson, J.L., Lindinger, N.M., Dodge, N.C., Molteno, C.D., Meintjes, E.M., Jacobson, S.W., 2017. Differential recruitment of brain regions during response inhibition in children prenatally exposed to alcohol. Alcohol Clin. Exp. Res. 41, 334–344.
Krauel, K., Duzel, E., Hinrichs, H., Santel, S., Rellum, T., Baving, L., 2007. Impact of emotional salience on episodic memory in attention-deficit/hyperactivity disorder: a functional magnetic resonance imaging study. Biol. Psychiat. 61, 1370–1379.
Lewis, C.E., Thomas, K.G.F., Dodge, N.C., Molteno, C.D., Meintjes, E.M., Jacobson, J.L., Jacobson, S.W., 2015. Verbal learning and memory impairment in children with fetal alcohol spectrum disorders. Alcohol Clin. Exp. Res. 39, 724–732.
Li, Z., Coles, C.D., Lynch, M.E., Ma, X., Peltier, S., Hu, X., 2008. Occipital-temporal reduction and sustained visual attention deficit in prenatal alcohol exposed adults. Brain Imaging Behav. 2, 39–48.
Maldjian, J.A., Laurienti, P.J., Kraft, R.A., Burdette, J.H., 2003. An automated method for neuroanatomic and cytoarchitectonic atlas-based interrogation of fMRI data sets. Neuroimage 19, 1233–1239.
Maldjian, J.A., Laurienti, P.J., Burdette, J.H., 2004. Precentral gyrus discrepancy in electronic versions of the Talairach atlas. Neuroimage 21, 450–455.
Malisza, K.L., Buss, J.L., Bolster, R.B., Dreessen de Gervai, P., Woods-Frohlich, L., Summers, R., Clancy, C.A., Chudley, A.E., Longstaffe, S., 2012. Comparison of spatial working memory in children with prenatal alcohol exposure and those diagnosed with ADHD: A functional magnetic resonance imaging study. J. Neurodev. Disord. 4, 1–20.
Maril, A., Avital, R., Reggev, N., Zuckerman, M., Sadeh, T., Ben Sira, L., Livneh, N., 2011. Event congruency and episodic encoding: a developmental fMRI study. Neuropsychologia 49, 3036–3045.
Mattson, S.N., Bernes, G.A., Doyle, L.R., 2019. Fetal alcohol spectrum disorders: A review of the neurobehavioral deficits associated with prenatal alcohol exposure. Alcohol Clin. Exp. Res. 43, 1046–1062.
Mattson, S.N., Riley, E.P., Delis, D.C., Stern, C., Jones, K.L., 1996. Verbal learning and memory in children with fetal alcohol syndrome. Alcohol Clin. Exp. Res. 20, 810–816.
Mattson, S.N., Roebuck, T.M., 2002. Acquisition and retention of verbal and nonverbal information in children with heavy prenatal alcohol exposure. Alcohol Clin. Exp. Res. 26, 875–882.
May, P.A., Blankenship, J., Marais, A.-S., Gossage, J.P., Kalberg, W.O., Barnard, R., De Vries, M., Robinson, L.K., Adnams, C.M., Buckley, D., Manning, M., Jones, K.L., Parry, C., Hoyme, H.E., Seedat, S., 2013. Approaching the prevalence of the full spectrum of fetal alcohol spectrum disorders in a South African population-based study. Alcohol. Clin. Exp. Res. 37, 818–830.
Meintjes, E.M., Jacobson, J.L., Molteno, C.D., Gatenby, J.C., Warton, C., Cannistraci, C. J., Hoyme, H.E., Robinson, L.K., Khaole, N., Gore, J.C., Jacobson, S.W., 2010. An fMRI study of number processing in children with fetal alcohol syndrome. Alcohol Clin. Exp. Res. 34, 1450–1464.
Meintjes, E.M., Narr, K.L., van der Kouwe, A.J.W., Molteno, C.D., Pirnia, T., Gutman, B., Woods, R.P., Thompson, P.M., Jacobson, J.L., Jacobson, S.W., 2014. A tensor-based morphometry analysis of regional differences in brain volume in relation to prenatal alcohol exposure. NeuroImage Clin. 5, 152–160.
Mick, E., Biederman, J., Faraone, S.V., Sayer, J., Kleinman, S., 2002. Case-control study of attention-deficit hyperactivity disorder and maternal smoking, alcohol use, and drug use during pregnancy. J. Am. Acad. Child Psy. 41, 378–385.
Moore, E.M., Migliorini, R., Infante, M.A., Riley, E.P., 2014. Fetal alcohol spectrum disorders: Recent neuroimaging findings. Curr. Dev. Disord. Rep. 1, 161–172.
Ofen, N., Kao, Y.-C., Sokol-Hessner, P., Kim, H., Whitfield-Gabrieli, S., Gabrieli, J.D.E., 2007. Development of the declarative memory system in the human brain. Nat. Neurosci. 10, 1198–1205.
Oldfield, R.C., 1971. The assessment and analysis of handedness: the Edinburgh inventory. Neuropsychologia 9, 97–113.
Pei, J.R., Rinaldi, C.M., Rasmussen, C., Massey, V., Massey, D., 2008. Memory patterns of acquisition and retention of verbal and nonverbal information in children with fetal alcohol spectrum disorders. Can. J. Clin. Parmacol. 15, e44–e56.
Roozen, S., Peters, G.-J.Y., Kok, G., Townend, D., Nijhuis, J., Curfs, L., 2016. Worldwide prevalence of fetal alcohol spectrum disorders: A systematic literature review including meta-analysis. Alcohol. Clin. Exp. Res. 40, 18–32.
Shing, Y.L., Brehmer, Y., Heekeren, H.R., Bäckman, L., Lindenberger, U., 2016. Neural activation patterns of successful episodic encoding: reorganization during childhood, maintenance in old age. Dev. Cogn. Neurosc. 20, 59–69.
Sowell, E.R., Lu, L.H., O'Hare, E.D., McCourt, S.T., Mattson, S.N., O'Connor, M.J., Bookheimer, S.Y., 2007. Functional magnetic resonance imaging of verbal learning in children with heavy prenatal alcohol exposure. NeuroReport 18, 635–639.
Tang, L., Pruitt, P.J., Yu, Q., Homayouni, R., Daugherty, A.M., Damoiseaux, J.S., Ofen, N., 2020. Differential functional connectivity in anterior and posterior hippocampus supporting the development of memory formation. Front. Hum. Neurosci. 14, 204.
Tang, L., Shafer, A.T., Ofen, N., 2018. Prefrontal cortex contributions to the development of memory formation. Cereb. Cortex 28, 3295–3308.
Tisdall, M.D., Hess, A., van der Kouwe, A.J.W., 2009. MPRAGE using EPI navigators for prospective motion correction. Proc. Int. Soc. Magn. Reson. Med. 17, 4656.
van der Kouwe, A.J.W., Benner, T., Salat, D.H., Fischl, B., 2008. Brain morphometry with multiecho MPRAGE. NeuroImage 40, 559–569.

Wagner, A.D., Schacter, D.L., Rotte, M., Koutstaal, W., Maril, A., Anders, M., Rosen, B.R., Buckner, R.L., 1998. Building memories: Remembering and forgetting of verbal experiences as predicted by brain activity. Science 281, 1188–1191.
Ware, A.L., Infante, M.A., O'Brien, J.W., Tapert, S.F., Jones, K.L., Riley, E.P., Mattson, S. N., 2015. An fMRI study of behavioral response inhibition in adolescents with and without histories of heavy prenatal alcohol exposure. Behav. Brain Res. 278, 137–146.
Wechsler, D., 2003. Wechsler Intelligence Scale for Children—Fourth edition. The Psychological Corporation, SanAntonio, TX.
Wilke, M., Holland, S.K., Altaye, M., Gaser, C., 2008. Template-o-matic: a toolbox for creating customized pediatric templates. NeuroImage 41, 903–913.
Winer, B.J., 1971. Statistical Principles in Experimental Design. McGraw-Hill, New York, NY.
Winocur, G., Moscovitch, M., Bontempi, B., 2010. Memory formation and long-term retention in humans and animals: Convergence towards a transformation account of hippocampal-neocortical interactions. Neuropsychologia. 48, 2339–2356.
Woods, K.J., Meintjes, E.M., Molteno, C.D., Jacobson, S.W., Jacobson, J.L., 2015. Parietal dysfunction during number processing in children with fetal alcohol spectrum disorders. NeuroImage Clin. 8, 594–605.